An exploration of the spatial scale over which orientation-dependent surround effects affect contour detection

Jennifer F. Schumacher Graduate Program in Neuroscience, University of Minnesota, USA

Christina F. Quinn Department of Psychology, University of Minnesota, USA

Cheryl A. Olman Department of Psychology, University of Minnesota, USA, & Department of Radiology, University of Minnesota, USA

Contour detection is a crucial component of visual processing; however, performance on contour detection tasks can vary depending on the context of the visual scene. S. C. Dakin and N. J. Baruch (2009) showed that detection of a contour in an array of distracting elements depends on the orientation of flanking elements. Here, using a line of five collinear Gabor elements ("target contour") in a field of distractor Gabor elements, we systematically measured the effects of eccentricity, spacing, and spatial frequency on contour detection performance in three different contexts: randomly oriented distractors (control condition), flanking distractors (on either side of the collinear Gabors) aligned approximately parallel to the target contour, and flanking distractors aligned approximately orthogonal to the target contour. In the control condition, contour detection performance was best for larger Gabors (2 cpd) spaced farther apart (1.2°). Parallel flankers reduced performance for intermediate and large spacings and sizes compared to the control condition, while orthogonal flankers increased performance for the smallest spacing and size compared to the control condition. The results are fit by a model in which collinear facilitation, which is size-dependent but can persist for several degrees of visual angle, competes with orientation-dependent suppression from the flanking context when elements are separated by less than a degree of visual angle.

Keywords: psychophysics, contour detection, contour integration, surround suppression, contextual modulation

Citation: Schumacher, J. F., Quinn, C. F., & Olman, C. A. (2011). An exploration of the spatial scale over which orientation-dependent surround effects affect contour detection. *Journal of Vision, 11*(8):12, 1–12, http://www.journalofvision.org/content/11/8/12, doi:10.1167/11.8.12.

Introduction

Local image context, the image features that surround the feature of interest, is an important factor that can either help or hinder one's performance in a visual task. Contour detection, in particular, is a task that depends strongly on the stimulus geometry and the spatial configuration of the visual scene (Bonneh & Sagi, 1998). In a contour detection task, Dakin and Baruch (2009) found that parallel context impaired contour detection performance, while an orthogonal context improved performance. Because both contour integration and orientation-dependent contextual modulation are known to operate over limited spatial scales, the experiment presented here was conducted in order to define the spatial scale over which each mechanism has the strongest effect.

Many studies have investigated possible neural mechanisms serving contour integration and detection. One mechanism in primary visual cortex (V1) that might contribute to contour integration is collinear facilitation: both detection thresholds and contrast discrimination thresholds are decreased for collinear elements (Cass & Alais, 2006; Cass & Spehar, 2005; Polat, 1999). A likely anatomical correlate for collinear facilitation in V1 involves the intrinsic horizontal connections between similar orientation columns (Bosking, Zhang, Schofield, & Fitzpatrick, 1997; Gilbert & Wiesel, 1989; Malach, Amir, Harel, & Grinvald, 1993; Rockland, Lund, & Humphrey, 1982). However, several lines of evidence indicate that contour integration relies on more than just collinear facilitation. For example, collinear facilitation occurs in more limited conditions than contour integration (Huang, Hess, & Dakin, 2006; Williams & Hess, 1998): While collinearity is important for correct and quick contour detection, about 20° of "jitter" (the amount of angular deviation from the contour axis) greatly impedes collinear facilitation but not contour detection (Williams & Hess, 1998). Other differences include: collinear facilitation and contour detection that are differentially affected by dichoptic presentation (Huang et al., 2006) and contours made of parallel elements ("ladders") that can be as salient as contours made of collinear elements ("snakes") (Bex, Simmers, & Dakin, 2001). Therefore,

doi: 10.1167/11.8.12 Received October 6, 2010; published July 21, 2011 ISSN 1534-7362

while collinear facilitation can be effectively modeled as a mechanism originating in striate cortex, models describing observers' performance on contour detection tasks generally rely on mechanisms with larger receptive fields and second-order contrast, such as orientation contrast (Dakin & Baruch, 2009; Field, Hayes, & Hess, 1993; May & Hess, 2008), which are generally attributed to extrastriate cortical areas.

A well-characterized visual context effect is orientation-dependent surround suppression: The response to a single element or to several collinear Gabor elements is often suppressed by a parallel surround but not by an orthogonal surround (or the orthogonal surround suppresses more weakly than a parallel surround or the orthogonal surround provides a release from suppression; Dakin & Baruch, 2009; Knierim & van Essen, 1992; Nothdurft, Gallant, & Van Essen, 1999; Solomon & Morgan, 2000; Zenger-Landolt & Koch, 2001). While intrinsic connections in V1 extend only about 2–4 mm on cortex (Amir, Harel, & Malach, 1993; Angelucci et al., 2002; Blasdel, Lund, & Fitzpatrick, 1985; Grinvald, Lieke, Frostig, & Hildesheim, 1994; Hupe et al., 1998), orientation-dependent surround effects can originate from context separated by 6–9 mm on cortex (Angelucci et al., 2002). As mentioned above for contour integration, this large spatial scale suggests an extrastriate origin for orientation-dependent surround effects, although this is an open area of research. Regardless of whether the cortical mechanisms are striate or extrastriate, the fact that both orientation-dependent surround suppression and contour integration depend strongly on eccentricity, spacing, spatial frequency, and stimulus contrast between the elements (Angelucci et al., 2002; Dakin & Baruch, 2009; Shani & Sagi, 2005) suggests that both of these contextual effects are mediated by visual mechanisms in relatively low-level retinotopic visual cortex.

For the present study, contour detection within a field of randomly oriented distractors provided a baseline against which orientation-dependent surround effects on contour detection could be measured. Our investigation of contour detection with orientation-dependent surround effects was designed to systematically characterize contour detection performance for a range of Gabor element spacings, sizes, and eccentricities to reveal the balance of contour integration and orientation-dependent suppression for visual elements separated by 0.6°–1.6° of visual angle.

Methods and materials

Subjects

Data were collected from seven subjects (four females, age 21–37, mean age 26.9) with normal or corrected-to-normal vision. The experimental protocols were approved by the Institutional Review Board at the University of Minnesota. Subjects provided written informed consent before participating in the experiments.

Stimuli

Stimuli were generated and presented with MATLAB (Mathworks, Natick, MA) and Psychtoolbox (Brainard, 1997; Pelli, 1997) and an iMac computer with OS X served as the processor. Stimuli were displayed on an NEC 2180UX LCD monitor, subtending 18.7 × 24.5 degrees of visual angle at a viewing distance of 100 cm. The screen luminance was measured with a photometer (Minolta CS-100, Konica-Minolta, Ramsey, NY) to generate a lookup table that produced linear brightness response on this monitor.

The stimuli consisted of a constant-size field of Gabor patches (total angular subtent: 11.7°) composed of a rectangular grid of distractor elements, the number of which varied as the spacing between the Gabors changed. Each Gabor patch consisted of a sinusoidal grating (2, 3.3, or 4 cpd) modulated by a Gaussian envelope, the width of which varied with spatial frequency (σ = 0.33/spatial frequency). Gabors were always presented at 80% contrast on a mean gray background. Phase was randomized, as previous work has shown that phase polarity does not affect contour integration in the fovea or near periphery (Hess & Field, 1999). A white square at the center of the field served as the fixation mark.

The target contour was a vertical line of five Gabors ("collinear Gabors"), which could occur either to the left or to the right of fixation on a given trial. For each trial, the orientation of the collinear Gabors was randomly selected to be one of six levels of orientation jitter, ranging from 0 to $\pm\pi/4$ radians. For all conditions, the orientations of the distractor elements were drawn from a uniform distribution [0 π], but relative orientation of neighboring distractors was controlled to avoid collinearities (i.e., orientation for a given element was redrawn from the distribution if $\Delta\theta < \pi/6$ when compared against 4 neighbors, one in each cardinal direction). For the control condition, the orientation of the elements on either side of the collinear Gabors was drawn from the same distribution as the rest of the distractor array. For the "parallel" condition, the orientation of the flanking distractor elements was drawn from a distribution of orientations parallel to the target Gabors (uniformly distributed, [$-\pi/4$ $\pi/4$], where 0 is vertical). For the "orthogonal" condition, the orientation of the flanking distractor elements was drawn from a distribution of orientations orthogonal to the target Gabors (uniformly distributed, [$\pi/4$ $3\pi/4$]). In the parallel and orthogonal conditions, the two flanking lines were present on both sides of the visual field, flanking both possible positions for the target collinear Gabors, on every trial. Three stimulus exemplars are shown in Figure 1.

Seven eccentricites (1.2°, 1.6°, 1.8°, 2.4°, 3°, 3.2°, 3.6°), three spacings (0.6°, 0.8°, 1.2°), and three spatial

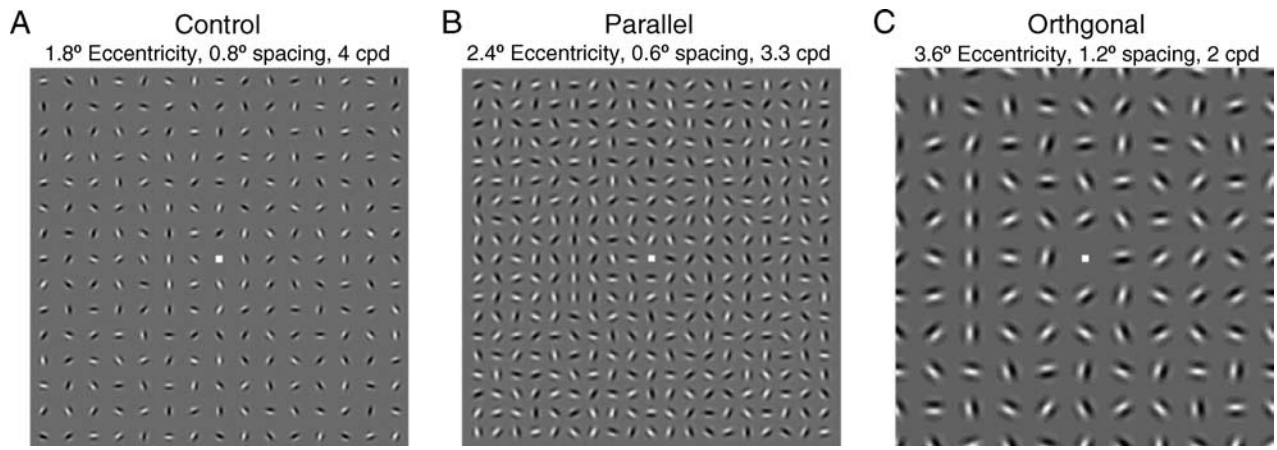

Figure 1. Examples of stimuli with collinear Gabors present on the left side. (A) Control condition (randomly oriented flanking distractors): in this example, the target contour is present at 1.6° eccentricity, with 4 cpd Gabors at 0.8° spacing. (B) Parallel condition: in this example, the target contour is present at 2.4° eccentricity, with 3.3 cpd Gabors at 0.6° spacing. (C) Orthogonal condition: in this example, the target contour is present at 3.6° eccentricity, with 2 cpd Gabors at 1.2° spacing.

frequencies (2 cycles per degree (cpd), 3.3 cpd, 4 cpd) defined the parameter space for our stimulus configurations; contour detection performance was measured for eighteen specific combinations from this parameter space. Figure 2 displays several views of the three-dimensional parameter space used for these experiments. For each combination of eccentricity, spatial frequency, and spacing, performance was measured in three conditions: control, parallel, and orthogonal.

Psychophysics

In a two-alternative forced-choice (2AFC) paradigm, subjects responded "left" or "right" to indicate where the (jittered) contour appeared. The stimulus was presented for 150 ms on each trial with unlimited time for subjects to respond and a 500-ms pause after the response and before the onset of the next trial. A gray screen was presented during the response period and intertrial interval. Subjects maintained fixation on the fixation square at the center of the screen; feedback was given by the fixation mark turning green for a correct response and red for an incorrect response. The fixation mark disappeared in between trials.

Tolerance to orientation jitter was measured using the method of constant stimuli. The eccentricity at which the collinear Gabors were presented, the spacing between the Gabor elements, and the spatial frequency of the Gabor patches were constant throughout each block of trials. One block contained 25 trials for each of 6 jitter levels for each of 3 contexts, for a total of 450 trials presented in random order per block. Each subject completed 2 repetitions of 18 configurations (blocks of trials). Psychometric functions for each stimulus condition and context (54 total thresholds—3 contexts for each of 18 configurations) were estimated from each subject's performance.

Analysis

Psychometric functions were fit with the Psignifit Matlab toolbox (version 2.5.6; see http://bootstrap-software.org/psignifit/), which is based on Wichmann

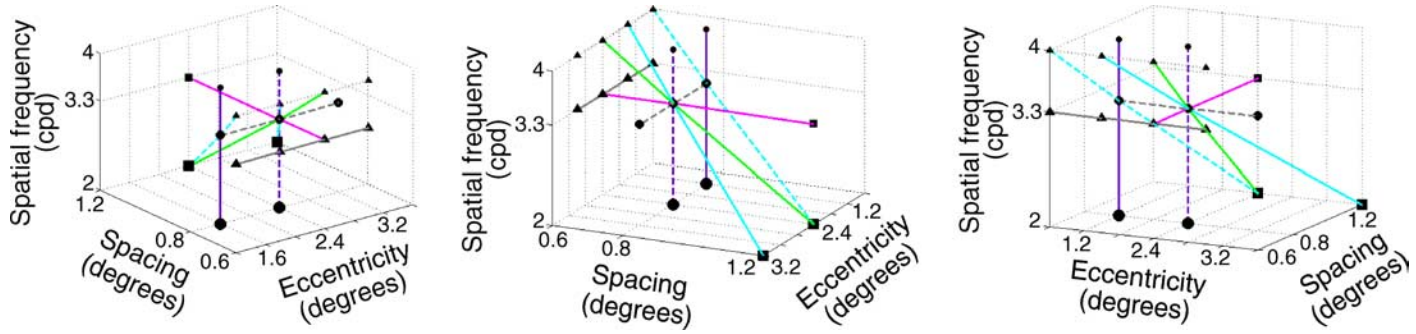

Figure 2. Representation of parameter space covered by these experiments. Color-coded lines indicate comparisons shown in Figures 4–6. Marker shapes indicate spacing (0.6°: triangle, 0.8°: circle, and 1.2°: square); marker sizes indicate spatial frequency (larger markers for lower spatial frequencies). Three views are given to help visualize the three-dimensional space.

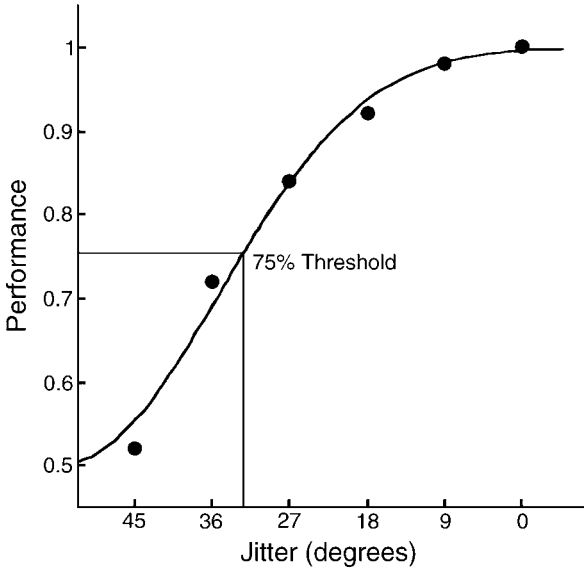

Figure 3. Typical psychometric function (control context, 1.2° eccentricity, 0.6° spacing, 3.3 cpd, subject 1). Percent correct is plotted for six levels of jitter, along with the Weibull function fit to data using maximum-likelihood estimation.

and Hill (2001). Performance over six levels of jitter was fit with a Weibull function using maximum-likelihood estimation (Figure 3). Thresholds were taken from the 75% correct fitted point. One subject's thresholds were significantly lower than the other six subjects, so this subject was excluded from further analysis. Thresholds were then averaged over the remaining six subjects per stimulus type and condition. Additionally, relative suppression indices for the parallel and control conditions were obtained by subtracting the parallel or control threshold from the orthogonal threshold per subject, then averaging.

Equation 1 shows the general form of a family of models that was tested to describe the contour integration and orientation-dependent surround effects we observed: T is the measured threshold, T_0 is a baseline constant, F is a function describing facilitation due to collinearity, and M is a function describing the strength of the surround effects:

$$T = T_0 + F - M. \quad (1)$$

The F and M terms are not physiologically plausible for separations less than the receptive field size; otherwise (particularly in the case of M), the equation would describe self-facilitation and self-masking. This model is therefore conceptualized as addressing only facilitation and masking arising outside a neuron's receptive field; correspondingly, data with spacing <0.6° were not measured or fit.

Several functional forms were tested for both F and M, using either exponential or Gaussian shapes as a function of either spacing (spc, in units of degrees) or spacing normalized by element carrier frequency (spc_{rel}, in units of λ). All models had six free parameters; the best fit (measured by sum of squared errors) was obtained with the following functional form:

$$T = T_0 + c_{\text{f}} e^{-\frac{\text{spc}_{\text{rel}}^2}{2\sigma_{\text{f}}^2}} + c_{\text{m}} e^{\frac{-\text{spc}}{\Delta_{\text{m}}}} \quad (2)$$

with

$$\Delta_{\text{m}} = c_1 + c_2 \cos^2(\theta_{\text{rel}}). \quad (3)$$

In Equation 2, the spatial scale, Δ_{m}, of the masking term depends on the average orientation of the flankers relative to the target contour (θ_{rel} = 0, π/4, or π/2) but also has an orientation-independent term (c_1). Models in which $\cos^2(\theta_{\text{rel}})$ modulated the amplitude, rather than the spatial extent, of the surround effect term were also tested but did not fit the data as well as the model presented above.

Results

We measured human subjects' performance for contour detection in three contexts (control, parallel, and orthogonal—referring to the orientation of the distractor Gabor elements immediately adjacent to the target contour) at eighteen different stimulus configurations differing in eccentricity, spacing, and spatial frequency. The degree of jitter at which a subject could distinguish the target contour from a line of randomly oriented Gabor elements with 75% accuracy was used to evaluate the subjects' threshold (tolerance for orientation jitter) in a contour detection task.

The control condition had randomly oriented distractors flanking the contour and is most similar to previous contour detection research. Performance was better for 0.8° separation than for 0.6° separation (dashed line versus solid line) but in all cases decreased as eccentricity increased (Figure 4A). No difference in performance was seen across spatial frequency (Figure 4C), consistent with previous work (Dakin & Hess, 1998). However, in contradiction to previous reports (Hess & Dakin, 1997), contour detection was not scale invariant: for a fixed eccentricity, performance increased significantly as spacing increased, even though size also increased so that relative spacing was constant (Figure 4D; $F_{2,15}$ = 12, p = 0.0008, ANOVA). Similarly, the increase in performance was also significant as spacing, spatial frequency, and eccentricity increased (Figure 4E; $F_{2,30}$ = 4.85, p = 0.015 across spacing and spatial frequency conditions; non-significant results for the interaction and no main effect

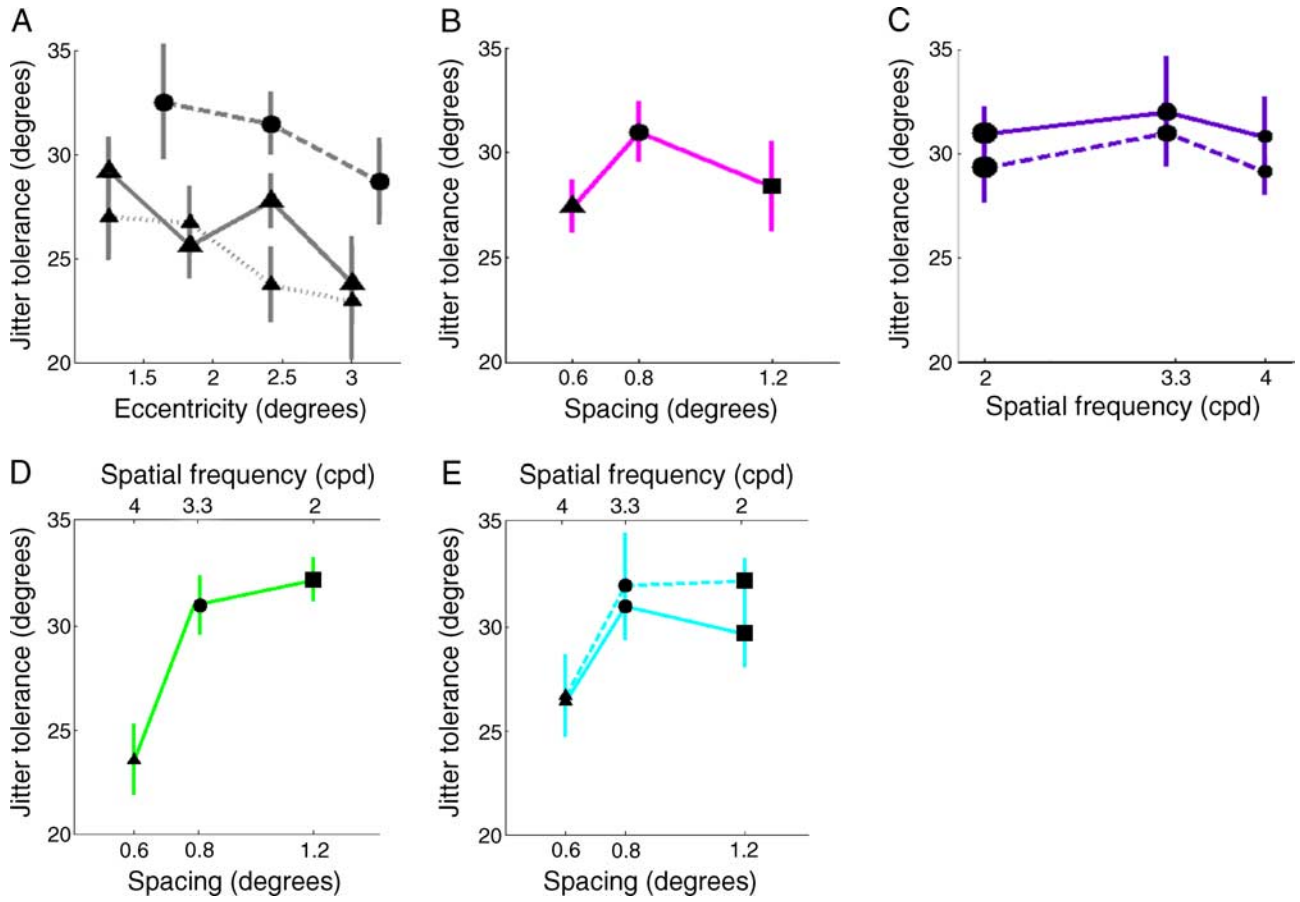

Figure 4. Control condition results. (A) Performance as a function of eccentricity. Solid line is 0.6° spacing and 3.3 cpd, dashed line is 0.8° spacing and 3.3 cpd, and dotted line is 0.6° spacing and 4 cpd. (B) Performance as a function of spacing for 3.3 cpd Gabors at 2.4° eccentricity. (C) Performance as a function of element size, for elements spaced at 0.8° with target contours at 1.6° eccentricity (solid line) and 2.4° eccentricity (dashed line). (D) At 2.4° eccentricity, performance significantly increased ($F_{2,15}$ = 12, p = 0.0008, ANOVA) as the elements were spaced further apart and were larger in size (relative spacing: 2.4λ–2.6λ). (E) Performance improved as elements were moved toward the periphery and scaled according to cortical magnification ($F_{2,30}$ = 4.85, p = 0.015, 2-way ANOVA). The solid line covered eccentricities of 1.2°, 1.6°, and 2.4° (relative spacing as in (D)), while the dashed line covered eccentricities of 1.8°, 2.4°, and 3.6°. Error bars in all panels are *SEM* (n = 6).

of eccentricity (solid line versus dotted line), 2-way ANOVA).

The orthogonal condition is the condition in which any orientation-tuned suppression from the flanking context should be minimized. Indeed, the tolerance to orientation jitter in the orthogonal condition was improved over the control condition for most configurations. Unlike the control condition, performance was relatively consistent across eccentricity when the target contour was flanked by orthogonal distractors (Figure 5A). Performance overall weakly decreased with an increase in spacing and also decreased with an increase in spatial frequency, for a fixed spacing (Figures 5B and 5C). The decrease in performance with an increase in spatial frequency is significant ($F_{2,30}$ = 3.83, p = 0.033 across spatial frequency; non-significant results for the interaction and no main effect of eccentricity (solid and dotted lines), 2-way ANOVA, Figure 5C).

Finally, the parallel condition is the condition in which any iso-orientation suppression effects should be largest. Performance during the parallel condition was always worse than performance on the orthogonal or control conditions. Data from the parallel condition are shown in Figure 6, along with data from the control condition, in the form of suppression indices calculated relative to the performance on the orthogonal task. The greatest effect of orientation-dependent suppression is seen at the closest spacings and lowest spatial frequencies (Figures 6B and 6C).

The observed pattern of results at 2.4° eccentricity was fit by a combination of contour integration and orientation-dependent surround effects to predict observers' contour detection thresholds, as a function of element size and spacing, and flanker orientation. Measured thresholds for seven stimulus configurations (21 conditions) are shown in Figure 7 along with thresholds predicted by the model. While none of the models tested

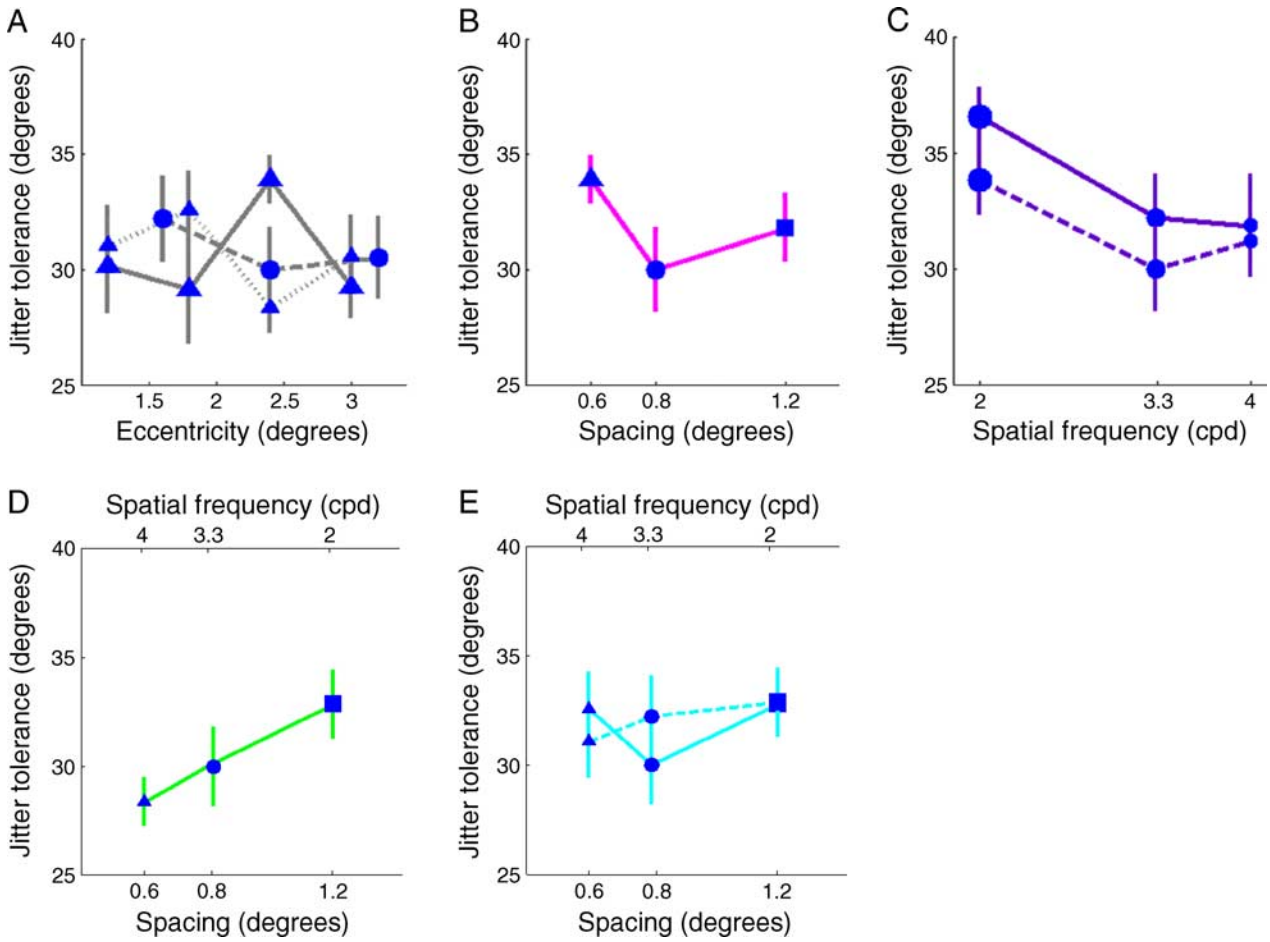

Figure 5. Orthogonal context results. Data are plotted as in Figure 4. The decrease in performance over spatial frequency (C) was statistically significant ($F_{2,30}$ = 3.83, p = 0.033, 2-way ANOVA).

(see Methods and materials section) provided a perfect fit to the data, the best-fitting model (Table 1) exhibits an interaction between relative spacing and flanker orientation similar to that observed in the data (Figure 7B, bottom right): thresholds for the control condition are closer to the parallel condition for close spacings but closer to the orthogonal condition for the largest spacing. This z-shaped pattern describes a system in which orientation-dependent surround effects dominate at close spatial scales but persist only for the parallel context when elements are separated by 0.8° or more. The characteristic space constant (Δ_m) in the parallel condition at 2.4° eccentricity was 0.65°, which corresponds to approximately 4–5 mm across the cortical surface in V1, assuming typical human cortical magnification (Engel, Glover, & Wandell, 1997). This spatial scale is consistent with other observations of orientation-dependent surround suppression (Angelucci et al., 2002) but on the high end of values typically reported for intrinsic inhibitory connections in V1. The modeled σ_f for the collinear facilitation term was even larger: 3.4, therefore ranging from 0.9° to 1.8°, which at 2.4° would span 6–12 mm in V1.

Discussion

This systematic study of contour detection performance as a function of element size, spacing, and flanking context extends our understanding of the interplay between contour integration and orientation-dependent suppressive surround effects. In the control condition, our data are largely consistent with previous reports: performance was consistent over the range of 2–4 cpd (Dakin & Hess, 1998; May & Hess, 2008) and decreased with increasing eccentricity. Our results differ from Dakin and Hess (1998) in that contour detection performance was not scale invariant, but as discussed below, this is likely due to the relatively small element separation used in these experiments. We have also replicated the orientation-dependent flanker effects from Dakin and Baruch (2009). However, our results extend previous work to show that the size and spacing of the Gabor elements determines whether orthogonal flankers will confer a detection advantage or parallel flankers will impair performance. A simple computational model

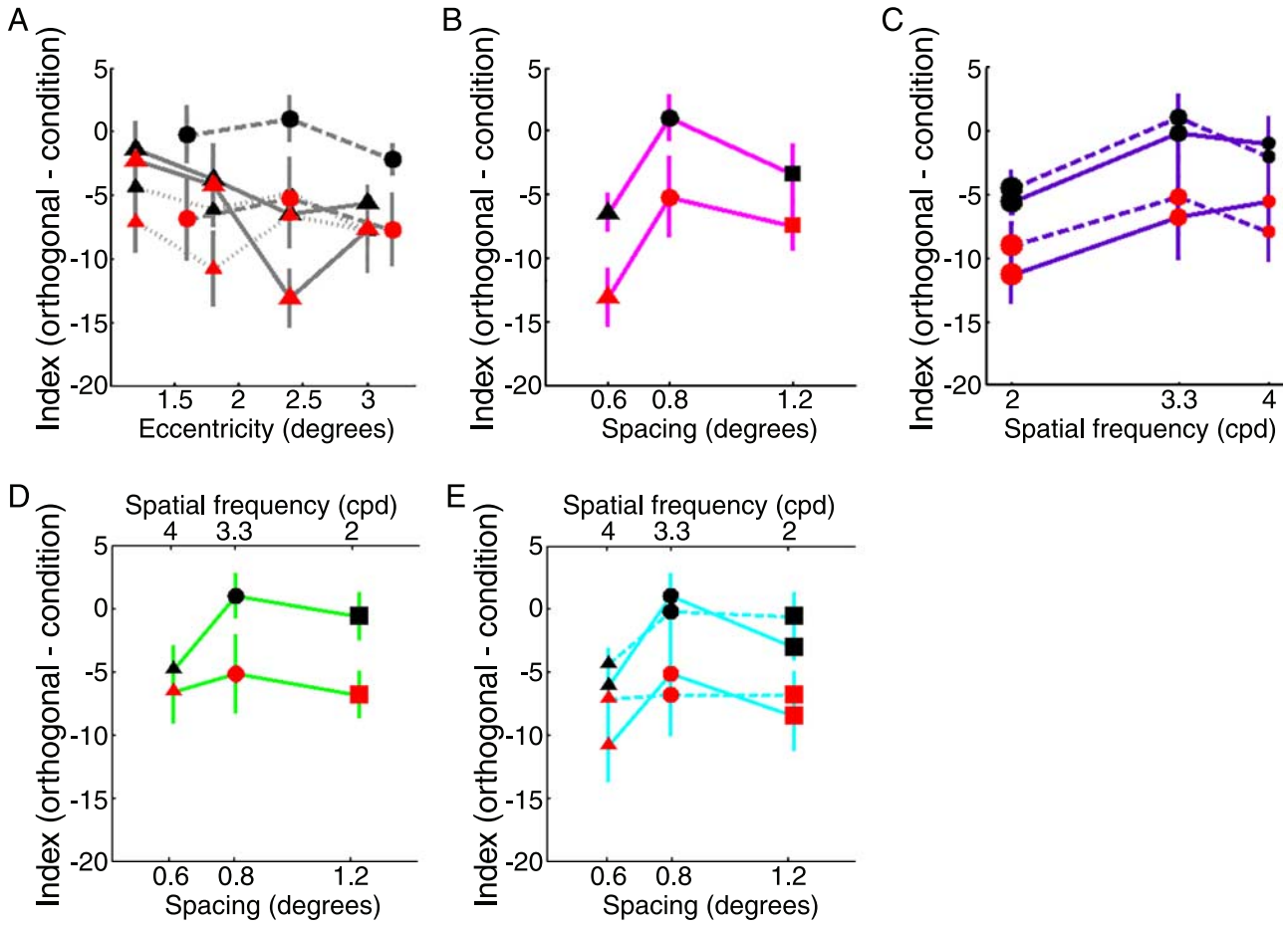

Figure 6. Performance on control and parallel conditions relative to orthogonal condition. Indices were calculated by subtracting thresholds in the control or parallel conditions from the thresholds of the orthogonal condition. Black markers represent the control condition and red markers indicate the parallel condition. Results are grouped as in Figure 4. Suppression indices for the control condition depended significantly on (B) spacing ($F_{2,15}$ = 3.73, p = 0.049, ANOVA) and (C) spatial frequency ($F_{2,30}$ = 5.5, p = 0.0092, 2-way ANOVA). Performance on the control condition also depended significantly on (E) scaling with eccentricity ($F_{2,30}$ = 6.51, p = 0.0045, 2-way ANOVA).

interpreting these data suggests that performance is determined by a balance of contour integration with orientation-dependent surround effects as spacing and spatial frequency interact.

The orthogonal condition minimizes orientation-dependent flanker effects, thus serving as a baseline for estimating contour integration performance as it depends on element spacing. In keeping with previous models of contour integration as a mechanism that operates at a relatively coarse spatial scale (Dakin & Baruch, 2009; Field et al., 1993; May & Hess, 2008; Mundenk & Itti, 2005), performance in the orthogonal condition generally depended weakly on element spacing and was the best for the largest Gabor elements. An interesting finding is the size dependence of performance on the contour detection task that is evident for the orthogonal condition (Figure 5C) but absent for the control condition and largely absent in previously published literature. One possible interpretation of this finding is that the orthogonal context unmasks size dependence in the contour integration mechanism (which should be present at a fixed spacing if the mechanism scales with relative spacing, as modeled in this and previous work). According to this interpretation, the size dependence would not be evident in the control condition because, even though relative spacing is increasing with element size, larger elements are also providing greater orientation-dependent suppression at the smaller relative spacings. However, our data for the parallel condition do not support this interpretation: performance is consistently poor for all sizes (Figure 7B, lower right panel), which indicates strong orientation-dependent effects for all sizes, not just the larger size. Because of the data from the parallel conditions, models with size-dependent terms (see Methods and materials section) for the orientation-dependent suppression did an inferior job of fitting the overall pattern of results. Therefore, our model fails to capture the apparent lack of size dependence in the control condition (Figure 7B, lower left panel) and we are unable at this point to provide a good mechanistic explanation for the novel finding of size dependence in the orthogonal condition when it is absent in the control condition.

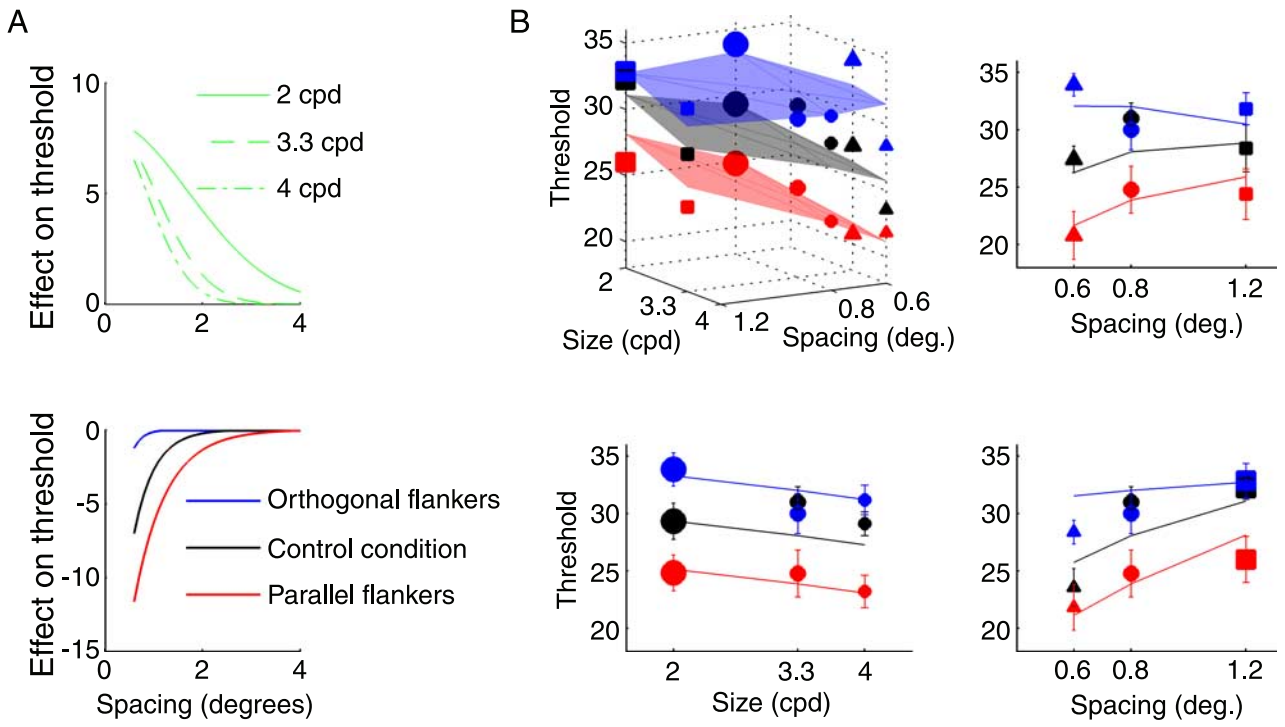

Figure 7. A computational model predicting observer performance as a balance between subtractive orientation-dependent lateral masking and additive size-dependent contour integration terms. (A) Model components describing collinear facilitation (green) and orientation-dependent lateral masking (blue: orthogonal flankers; black: control condition; red: parallel flankers) are plotted as a function of element spacing in the visual field. The best fit to the data was obtained, modeling collinear facilitation as a function of *relative* spacing but orientation-dependent suppression as a function of *absolute* spacing. (B) The 3D plot in the upper left shows modeled thresholds (shaded surfaces) and measured thresholds (shapes and sizes of data points indicate size and spacing as in Figures 4–6; color indicates flanker orientation) for all conditions at 2.4° eccentricity. The other three panels show slices through this 3D space, with solid lines indicating model fits; error bars on data points are *SEM* across 6 subjects.

The control condition can be viewed as intermediate between orthogonal and parallel conditions—the average orientation of the flanking context is $\pi/4$, relative to the contour elements. Consistent with this view, performance in the control condition was always bounded by performance on the parallel and orthogonal conditions. The orientation-dependent surround effects that reduced performance on the control and parallel conditions (relative to the orthogonal condition) depended strongly on the spacing and spatial frequency of the elements, decreasing both with increased separation between the individual elements and with decreased size (Figures 6B and 6C). Both increased separation and decreased size result in an increased cortical distance between the elements, suggesting that orientation-dependent surround effects depend critically on the distance between cortical representations of stimuli. The dependence of orientation-dependent surround effects on eccentricity (the orthogonal condition showed no effect of eccentricity, while performance on the control and parallel conditions decreased as the contour was placed further in the periphery; Figure 6A) is also consistent with a mechanism that operates over a limited cortical scale and spans a larger angular subtent as cortical magnification decreases. By the same logic, the lack of eccentricity dependence in the orthogonal condition is consistent with a contour integration mechanism that operates over a relatively large spatial scale.

One way in which these experiments fail to replicate results from the literature is that we observe a lack of scale invariance in the control condition (Figure 4C). In previous studies, performance has remained consistent as elements were increased in size and the spacing was correspondingly scaled (Hess & Dakin, 1997). This scale invariance should persist to 4° of eccentricity, beyond which the differences between foveal and peripheral performance have been attributed to differences in spatial attention (Field et al., 1993; Hess & Dakin, 1997; Ito & Gilbert, 1999; Shani & Sagi, 2005). In our study, performance approached scale invariance in the orthogonal condition when eccentricity was also increased to

	Parameter					
	T_0	c_f	σ_f	c_m	c_1	c_2
Value	26	8.3	3.4	29	0.19	0.46

Table 1. Parameters for the model (Equations 2 and 3) to fit the data as shown in Figure 7.

match the scaling of size and spacing (Figure 5E) but not in the control or parallel condition. The fact that we observed scale invariance in the orthogonal condition, in which orientation-dependent suppressive effects from the flanking context are minimized, suggests that our data on the control and parallel conditions might diverge from the published literature because the average spacing between the elements was smaller than in previous experiments. Indeed, Hess and Dakin (1997) used a spacing of about 4λ when they reported scale invariance; we only tested scale invariance for relative spacings near 2.4λ, and the smaller relative spacing likely increases the importance of suppressive surround effects.

An important difference between our design and many contour detection tasks reported in the literature is that our task is not a search task. While we held the total stimulus subtent constant, previous experiments testing for scale invariance fixed the number of distractor elements—an important control in a search task. To test whether the variability in the number of distractor elements affected our results, 4 subjects completed a follow-up experiment collecting the data from Figure 6D with the number of elements fixed instead of the grid size fixed. The results for the two variations (grid size constant vs. number of elements constant; Figure 8) are almost identical, indicating that the lack of scale invariance we measure is not a consequence of the variation in the number of total elements in the image. This lack of scale invariance might be attributed to the particular balance of orientation-dependent suppression and facilitation from contour integration at this range of spacings and sizes. While we were collecting these control data, we also collected data on an additional point at a larger spacing (1.6°) and smaller spatial frequency (1.5 cpd). As spacing increases, the difference between the orthogonal and parallel conditions continues to decrease, which is consistent with orientation-dependent suppression effects operating over a more limited spatial range than contour integration effects (performance on the orthogonal condition remains high as spacing increases).

While other research has shown a decrease in performance with an increase in spacing, our data and model show a weak decrease, if any, for the orthogonal condition (fixed element size; Figure 7B, upper right panel) and an increase in performance for the parallel condition. May and Hess (2008) found that contour detection performance decreased with increasing spacing when element separations ranged from about 1° to 3°; Field et al. (1993) used spacings between 0.25° and 0.9°, which overlaps with our spacings of 0.6°–1.2°, and found a decrease in performance with increasing spacing. To understand how our work compares against these previous studies, we fit a second model to our data that could account for change in performance with eccentricity. To do this, we scaled the element spacing by the square root of the eccentricity (e.g., entering 0.6°/√2.4° into Equation 2 for spc, instead of just 0.6°; spc_{rel} was calculated as, e.g., spc/√(ecc/λ)) and fit all 54 data points from the 18 stimulus configurations. This was not presented in Figure 7 as the main model because we lack *a priori* justification for using the square root of eccentricity to scale the spacing; of the scaling functions we tested, it simply was the one that allowed us to use a model otherwise identical to that shown in Equations 1–3 to fit all the data with reasonable parameter values and no systematic biases. With this modification, the fit to all 54 data points (fit parameters

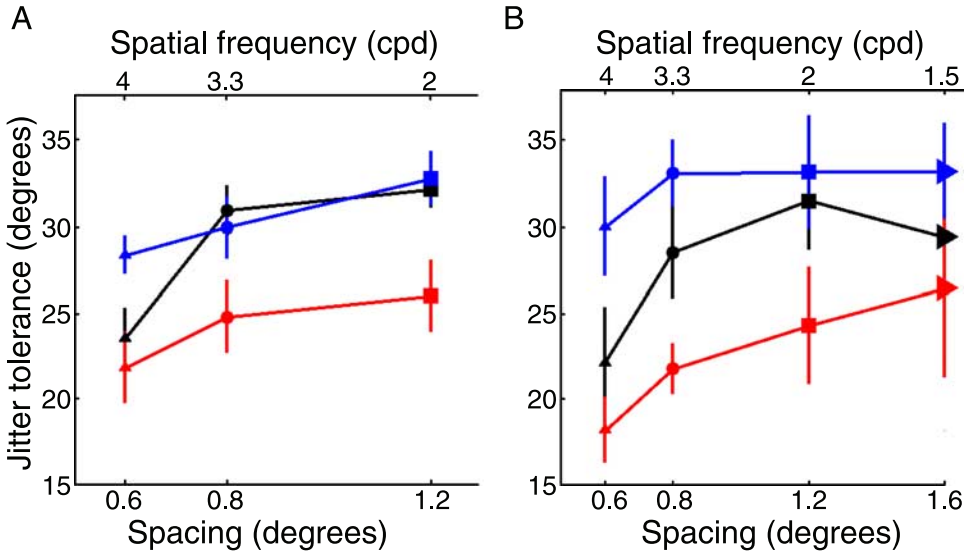

Figure 8. Comparison of results for constant grid size with variable Gabor element number and constant Gabor element number with variable grid size. (A) Constant grid size, as shown in Figure 7B (n = 6 subjects). (B) Constant Gabor element number. Blue: orthogonal, black: control, red: parallel flankers. Rightward-pointing triangles indicate 1.5 cpd elements separated by 1.6°. Error bars are *SEM* (n = 4 except the condition with 1.6° spacing and 1.5 cpd, for which n = 3).

	Parameter					
	T_0	c_f	σ_f	c_m	c_1	c_2
Value	21	14	4.2	26	0.18	0.31

Table 2. Parameters for the model (Equations 2 and 3) to fit all 54 data points with spacing scaled by eccentricity.

shown in Table 2) was actually better than the model fit to the 21 data points at 2.4° eccentricity (average difference between modeled and fit thresholds was 0.22 vs. 0.33). With this ability to predict performance at a range of eccentricities, we can consider whether our model is applicable to typical contour detection studies in which stimuli are presented closer to the fovea or subjects are searching for the contour (free-viewing). Specifically for the study reported by Field et al. (1993), because the (eccentricity-scaled) relative spacing is large near the fovea, the eccentricity-scaled version of our model predicts decreased performance with increasing spacing for the 8 cpd Gabors separated by 0.25°–0.9° at ~1° eccentricity in Field et al. However, the eccentricity-scaled version of the model still predicts an *increase* in performance with an increase in element spacing (interpreted as a release from short-range, orientation-tuned suppression effects) for the stimuli tested in Field et al. if the flanking context were to be parallel; future work will test this prediction to verify extensibility of our work to free-viewing of contours.

Interestingly, with visual stimuli quite different from ours, using simple tilted or vertical bars as target elements and distractors, a similar spatial scale for the effect of parallel or orthogonal elements on visual search was reported (May & Zhaoping, 2009). A target bar was placed 1°–4° from an axis that was aligned parallel or orthogonal to the target and distractors. Our findings would predict a decrement in performance with the parallel axis up to about 2.5° (Figure 7A, lower panel), which is what May and Zhaoping (2009) observed. Our findings would also predict no suppressive effect from the orthogonal axis within this spatial range (equal to or greater than 1° separation) and they also saw no suppressive effect in this range with an orthogonal axis.

While the general ideas captured by the computational model shown in Figure 7 are informative, and confidence in the conclusions is bolstered where they are supported by previous literature, the model did not capture all of the observed behavior—for example, the model underrepresents the similarity of the thresholds for the control and parallel conditions with small elements (4 cpd) that are closely spaced (0.6°, Figure 7B, lower right panel, although note that the data from the follow-up experiment in Figure 8B show good agreement with model predictions). The reason that the model fails to fit this particular pair of points is that it is also constrained to fit the data at 0.8° spacing, 4 cpd elements, where performance on the control condition was almost identical to performance on the *orthogonal* condition. We tried several other types of models, including full image models (multiple orientation and spatial frequency channels) similar to those shown in Dakin and Baruch (2009) and May and Hess (2008), but the other models did not do a better job of capturing this aspect of the observed performance. Thus, the estimated spatial scales for orientation-dependent lateral masking and contour integration can only be approximate, as the fits to the data are limited.

Another limitation of our design is that it cannot separately characterize the contributions of collinear facilitation and contour integration. A second experiment with "ladders" as well as "snakes" (Bex et al., 2001) would be required to allow separate characterization of the contribution of collinear facilitation to the contour detection performance we have measured. Thus, we have used the term "contour integration" to describe the facilitative term in our model, intending that this comprises a combination of low-level collinear facilitation and higher level mechanisms.

The primary finding of this work is that the orientation-dependent suppressive effects that inhibit contour integration appear to operate over a more limited spatial range than the facilitative mechanisms that serve contour integration. The pattern supporting this conclusion is most evident in Figure 7B. In the upper right panel, the effect of flanking context is reduced by half when the spacing is doubled, but performance on the contour detection task with orthogonal context (the condition in which flanking effects are minimized) decreases only slightly with the doubling in element spacing. This pattern suggests that, for our set of stimuli in which target elements and distractors are relatively dense, facilitative mechanisms aiding contour integration depend weakly on spacing while orientation-dependent suppressive mechanisms depend more strongly on spacing.

Conclusion

Contour integration and orientation-dependent flanker effects appear to operate on different spatial scales. In keeping with previous work on local contextual modulation in V1, we find that the spatial scale over which orientation-dependent lateral masking affects contour integration is potentially larger than can be supported by V1 intrinsic mechanisms. The still longer range of contour integration supports an extrastriate mechanism serving contour integration. The interplay between these two mechanisms indicates that previous findings such as scale invariance in contour detection performance will hold only over a particular range of element spacings and that observers' ability to detect contours in crowded environments is strongly dependent on local image context.

Acknowledgments

We thank Keith May and an anonymous reviewer for their helpful comments.

Commercial relationships: none.
Corresponding author: Jennifer F. Schumacher.
Email: schum204@umn.edu.
Address: 3M Center, 0235-03-F-08, St. Paul, MN 55144-1000, USA.

References

Amir, Y., Harel, M., & Malach, R. (1993). Cortical hierarchy reflected in the organization of intrinsic connections in macaque monkey visual cortex. *Journal of Comparative Neurology, 334,* 19–46.

Angelucci, A., Levitt, J. B., Walton, E. J., Hupe, J. M., Bullier, J., & Lund, J. S. (2002). Circuits for local and global signal integration in primary visual cortex. *Journal of Neuroscience, 22,* 8633–8646.

Bex, P. J., Simmers, A. J., & Dakin, S. C. (2001). Snakes and ladders: The contribution of temporal modulation to visual contour integration. *Vision Research, 41,* 3775–3782.

Blasdel, G. G., Lund, J. S., & Fitzpatrick, D. (1985). Intrinsic connections of macaque striate cortex: Axonal projections of cells outside lamina 4C. *Journal of Neuroscience, 5,* 3350–3369.

Bonneh, Y., & Sagi, D. (1998). Effects of spatial configuration on contrast detection. *Vision Research, 38,* 3541–3553.

Bosking, W. H., Zhang, Y., Schofield, B., & Fitzpatrick, D. (1997). Orientation selectivity and the arrangement of horizontal connections in tree shrew striate cortex. *Journal of Neuroscience, 17,* 2112–2127.

Brainard, D. H. (1997). The psychophysics toolbox. *Spatial Vision, 10,* 433–436.

Cass, J., & Alais, D. (2006). The mechanisms of collinear integration. *Journal of Vision, 6*(9):5, 915–922, http://www.journalofvision.org/content/6/9/5, doi:10.1167/6.9.5. [PubMed] [Article]

Cass, J. R., & Spehar, B. (2005). Dynamics of collinear contrast facilitation are consistent with long-range horizontal striate transmission. *Vision Research, 45,* 2728–2739.

Dakin, S. C., & Baruch, N. J. (2009). Context influences contour integration. *Journal of Vision, 9*(2):13, 1–13, http://www.journalofvision.org/content/9/2/13, doi:10.1167/9.2.13. [PubMed] [Article]

Dakin, S. C., & Hess, R. F. (1998). Spatial-frequency tuning of visual contour integration. *Journal of the Optical Society of America A, Optics, Image Science, and Vision, 15,* 1486–1499.

Engel, S. A., Glover, G. H., & Wandell, B. A. (1997). Retinotopic organization in human visual cortex and the spatial precision of functional MRI. *Cerebral Cortex, 7,* 181–192.

Field, D. J., Hayes, A., & Hess, R. F. (1993). Contour integration by the human visual system: Evidence for a local "association field". *Vision Research, 33,* 173–193.

Gilbert, C. D., & Wiesel, T. N. (1989). Columnar specificity of intrinsic horizontal and corticocortical connections in cat visual cortex. *Journal of Neuroscience, 9,* 2432–2442.

Grinvald, A., Lieke, E. E., Frostig, R. D., & Hildesheim, R. (1994). Cortical point-spread function and long-range lateral interactions revealed by real-time optical imaging of macaque monkey primary visual cortex. *Journal of Neuroscience, 14,* 2545–2568.

Hess, R., & Field, D. (1999). Integration of contours: New insights. *Trends in Cognitive Sciences, 3,* 480–486.

Hess, R. F., & Dakin, S. C. (1997). Absence of contour linking in peripheral vision. *Nature, 390,* 602–604.

Huang, P.-C., Hess, R. F., & Dakin, S. C. (2006). Flank facilitation and contour integration: Different sites. *Vision Research, 46,* 3699–3706.

Hupe, J. M., James, A. C., Payne, B. R., Lombe, S. G., Girard, P., & Bullier, J. (1998). Cortical feedback improves discrimination between figure and background by V1, V2 and V3 neurons. *Nature, 394,* 784–787.

Ito, M., & Gilbert, C. D. (1999). Attention modulates contextual influences in the primary visual cortex of alert monkeys. *Neuron, 22,* 593–604.

Knierim, J. J., & van Essen, D. C. (1992). Neuronal responses to static texture patterns in area V1 of the alert macaque monkey. *Journal of Neurophysiology, 67,* 961–980.

Malach, R., Amir, Y., Harel, M., & Grinvald, A. (1993). Relationship between intrinsic connections and functional architecture revealed by optical imaging and in vivo targeted biocytin injections in primate striate cortex. *Proceedings of the National Academy of Sciences of the United States of America, 90,* 10469–10473.

May, K. A., & Hess, R. F. (2008). Effects of element separation and carrier wavelength on detection of snakes and ladders: Implications for models of contour integration. *Journal of Vision, 8*(13):4, 1–23, http://www.journalofvision.org/content/8/13/4, doi:10.1167/8.13.4. [PubMed] [Article]

May, K. A., & Zhaoping, L. (2009). Effects of surrounding frame on visual search for vertical or tilted bars. *Journal*

of Vision, 9(13):20, 1–19, http://www.journalofvision.org/content/9/13/20, doi:10.1167/9.13.20. [PubMed] [Article]

Mundenk, T. N., & Itti, L. (2005). Computational modeling and exploration of contour integration for visual saliency. *Biological Cybernetics, 93,* 188–212.

Nothdurft, H. C., Gallant, J. L., & Van Essen, D. C. (1999). Response modulation by texture surround in primate area V1: Correlates of "popout" under anesthesia. *Visual Neuroscience, 16,* 15–34.

Pelli, D. G. (1997). The VideoToolbox software for visual psychophysics: Transforming numbers into movies. *Spatial Vision, 10,* 437–442.

Polat, U. (1999). Functional architecture of long-range perceptual interactions. *Spatial Vision, 12,* 143–162.

Rockland, K. S., Lund, J. S., & Humphrey, A. L. (1982). Anatomical binding of intrinsic connections in striate cortex of tree shrews (*Tupaia glis*). *Journal of Comparative Neurology, 209,* 41–58.

Shani, R., & Sagi, D. (2005). Eccentricity effects on lateral interactions. *Vision Research, 45,* 2009–2024.

Solomon, J. A., & Morgan, M. J. (2000). Facilitation from collinear flanks is cancelled by non-collinear flanks. *Vision Research, 40,* 279–286.

Wichmann, F. A., & Hill, N. J. (2001). The psychometric function: I. Fitting, sampling, and goodness of fit. *Perception & Psychophysics, 63,* 1293–1313.

Williams, C. B., & Hess, R. F. (1998). Relationship between facilitation at threshold and suprathreshold contour integration. *Journal of the Optical Society of America A, 15,* 2046–2051.

Zenger-Landolt, B., & Koch, C. (2001). Flanker effects in peripheral contrast discrimination—Psychophysics and modeling. *Vision Research, 41,* 3663–3675.